ARTICLES

Anaphase initiation is regulated by antagonistic ubiquitination and deubiquitination activities

Frank Stegmeier[1]*, Michael Rape[3]*†, Viji M. Draviam[3,4], Grzegorz Nalepa[2], Mathew E. Sowa[2], Xiaolu L. Ang[2], E. Robert McDonald III[1], Mamie Z. Li[1], Gregory J. Hannon[5], Peter K. Sorger[3,4], Marc W. Kirschner[3], J. Wade Harper[2] & Stephen J. Elledge[1]

The spindle checkpoint prevents chromosome mis-segregation by delaying sister chromatid separation until all chromosomes have achieved bipolar attachment to the mitotic spindle. Its operation is essential for accurate chromosome segregation, whereas its dysregulation can contribute to birth defects and tumorigenesis. The target of the spindle checkpoint is the anaphase-promoting complex (APC), a ubiquitin ligase that promotes sister chromatid separation and progression to anaphase. Using a short hairpin RNA screen targeting components of the ubiquitin-proteasome pathway in human cells, we identified the deubiquitinating enzyme USP44 (ubiquitin-specific protease 44) as a critical regulator of the spindle checkpoint. USP44 is not required for the initial recognition of unattached kinetochores and the subsequent recruitment of checkpoint components. Instead, it prevents the premature activation of the APC by stabilizing the APC-inhibitory Mad2–Cdc20 complex. USP44 deubiquitinates the APC coactivator Cdc20 both *in vitro* and *in vivo*, and thereby directly counteracts the APC-driven disassembly of Mad2–Cdc20 complexes (discussed in an accompanying paper). Our findings suggest that a dynamic balance of ubiquitination by the APC and deubiquitination by USP44 contributes to the generation of the switch-like transition controlling anaphase entry, analogous to the way that phosphorylation and dephosphorylation of Cdk1 by Wee1 and Cdc25 controls entry into mitosis.

Aneuploidy, a state of abnormal chromosome number, is a hallmark of aggressive tumours and can arise from errors during chromosome segregation[1–3]. Faithful chromosome segregation requires that each chromatid pair achieves bipolar attachment to the mitotic spindle before their segregation. Segregation is initiated by activation of the APC, an E3 ubiquitin ligase. When bound to its cofactor Cdc20, APC^{Cdc20} drives cells into anaphase by inducing the degradation of securin and mitotic cyclins[4]. The spindle checkpoint ensures that activation of the APC is delayed until all chromosomes have achieved bipolar kinetochore–microtubule attachment. Many checkpoint proteins are recruited to unattached kinetochores and are thought to facilitate the binding of Mad2 and BubR1 to Cdc20, thereby inhibiting APC^{Cdc20} activity[5–7].

The first spindle checkpoint components were discovered through genetic screens in budding yeast[8–10], and characterization of their metazoan orthologues showed the conservation of fundamental aspects of mitotic checkpoint signalling from yeast to human[3,6]. However, recent studies revealed that spindle checkpoint signalling is more complex in mammalian cells, as Zw10 (zeste-white 10), Rod (rough-deal) and $p31^{comet}$ regulate spindle checkpoint function in higher eukaryotes but lack clear yeast orthologues[11–15].

Here we use a genetic approach to identify novel regulators of spindle checkpoint control in human cells. By screening a short hairpin (sh)RNA library that targets genes in the ubiquitin-proteasome pathway, we have identified a previously uncharacterized deubiquitinating enzyme, USP44. We find that USP44 acts downstream of kinetochore-localized spindle checkpoint complexes and prevents premature activation of the APC by stabilizing the APC-inhibitory Mad2–Cdc20 complex. USP44 can directly deubiquitinate Cdc20 and counteract the APC-driven disassembly of spindle checkpoint complexes[16] both *in vitro* and *in vivo*. Our study indicates that spindle checkpoint regulation of the APC is based on a dynamic balance of counteracting ubiquitination and deubiquitination activities.

shRNA screen for spindle checkpoint regulators

Given that the central target of the spindle checkpoint is the APC[4–7], we wished to explore possible roles of other components of the ubiquitin pathway in the regulation of anaphase entry through the spindle checkpoint. Using a human microRNA-based genome-wide shRNA library as a source of hairpins[17], we developed an arrayed shRNA library containing 1,964 hairpins targeting 759 genes related to the ubiquitin pathway (see Supplementary Fig. 1b and Supplementary Table 1 for detailed library information). We screened this library for regulators of the spindle checkpoint using a high-throughput visual screening platform (Supplementary Fig. 1a–c). This screen was intended to identify two classes of genes whose depletion leads to a reduced mitotic index: (1) spindle checkpoint components, the inactivation of which by-passes Taxol-induced mitotic arrest; and (2) pre-mitotic cell-cycle regulators, the inactivation of which delays cells before mitotic entry. In contrast to the multi-lobed nuclear

[1]Howard Hughes Medical Institute, Department of Genetics, Harvard Partners Center for Genetics and Genomics, and [2]Department of Pathology, Harvard Medical School, 77 Avenue Louis Pasteur, Boston, Massachusetts 02115, USA. [3]Department of Systems Biology, Harvard Medical School, Boston, Massachusetts 02115, USA. [4]Department of Biology, Massachusetts Institute of Technology, Cambridge, Massachusetts 02139, USA. [5]Cold Spring Harbor Laboratory, Watson School of Biological Sciences, 1 Bungtown Road, Cold Spring Harbor, New York 11724, USA. †Present address: Department of Molecular and Cell Biology, University of California at Berkeley, Berkeley, California 94720-3202, USA.
*These authors contributed equally to this work.

©2007 Nature Publishing Group

morphology caused by checkpoint by-pass, cells that arrest before mitosis contained normal (unlobed) interphase nuclei, which allowed us to classify preliminarily our candidate genes into potential checkpoint regulators (MN for multi-lobed nuclei) and cell division cycle mutants (CDC, borrowing from the yeast nomenclature) (Supplementary Fig. 1d). Our screen identified known regulators of pre-mitotic cell-cycle progression (for example, *EMI1* (also called *FBXO5*) and *SKP2*) and 14 new candidate spindle checkpoint regulators and CDC mutants (Supplementary Fig. 1d). We validated the most penetrant candidate genes with additional siRNAs that target different regions within each gene (Fig. 1a, b and Supplementary Fig. 2), strengthening the notion that phenotypes are due to target downregulation rather than off-target effects.

We focused our investigation on the candidate checkpoint protein USP44, a previously uncharacterized deubiquitinating enzyme, because it had the most penetrant phenotype of all candidate spindle checkpoint regulators. Depletion of USP44 abolished checkpoint function in all three cell lines tested (Fig. 1 and Supplementary Fig. 3), and the efficiency in the reduction of USP44 levels for different siRNAs strongly correlated with their phenotypic penetrance in the checkpoint assay (Fig. 1a, d). Furthermore, expression of an siRNA-resistant version of USP44 rescued the spindle checkpoint defect of USP44-depleted cells (Fig. 1e, USP44(siRes)), confirming the specificity of our RNAi constructs. In contrast, a catalytically inactive USP44 mutant failed to restore spindle checkpoint function (Fig. 1e, USP44(ci-siRes)). Thus, deubiquitination mediated by USP44 is essential for spindle checkpoint function in human cells.

USP44 activity is elevated in mitosis

Consistent with an essential function of USP44 in the spindle checkpoint, USP44 levels were increased in mitotic cells (Fig. 2a), but rapidly decreased once cells had completed chromosome attachment and exited from mitosis (Fig. 2b). We noted the appearance of a slower migrating form of USP44 as cells entered mitosis (Fig. 2a) that disappeared shortly after release from nocodazole-mediated arrest and preceded USP44's degradation (Fig. 2b). This slower migrating form was also evident when recombinant USP44 was incubated in mitotic extracts, and became more pronounced after treatment with the phosphatase inhibitor okadaic acid, indicating that USP44 may be phosphorylated in mitosis (Fig. 2c).

To test whether the deubiquitination activity of USP44 is cell-cycle regulated, we took advantage of the fact that USP44 purified from insect cells has very low catalytic activity in an *in vitro* deubiquitination assay (Fig. 2d). Notably, pre-incubation of recombinant USP44 with extracts from nocodazole-arrested cells strongly increased the activity of USP44, whereas treatment with S-phase extracts resulted only in residual activation similar to a catalytically inactive mutant (Fig. 2d). Together, these findings indicate that USP44 is activated in checkpoint-arrested mitotic cells and rapidly degraded as cells exit from mitosis.

USP44 prevents premature anaphase onset

To characterize the mitotic function of USP44 in an unperturbed mitosis, we monitored mitotic progression and chromosome movement in USP44-depleted HeLa cells expressing histone H2B tagged with green fluorescent protein (GFP). Downregulation of USP44 led to a variety of mitotic defects, including the failure to form a clear

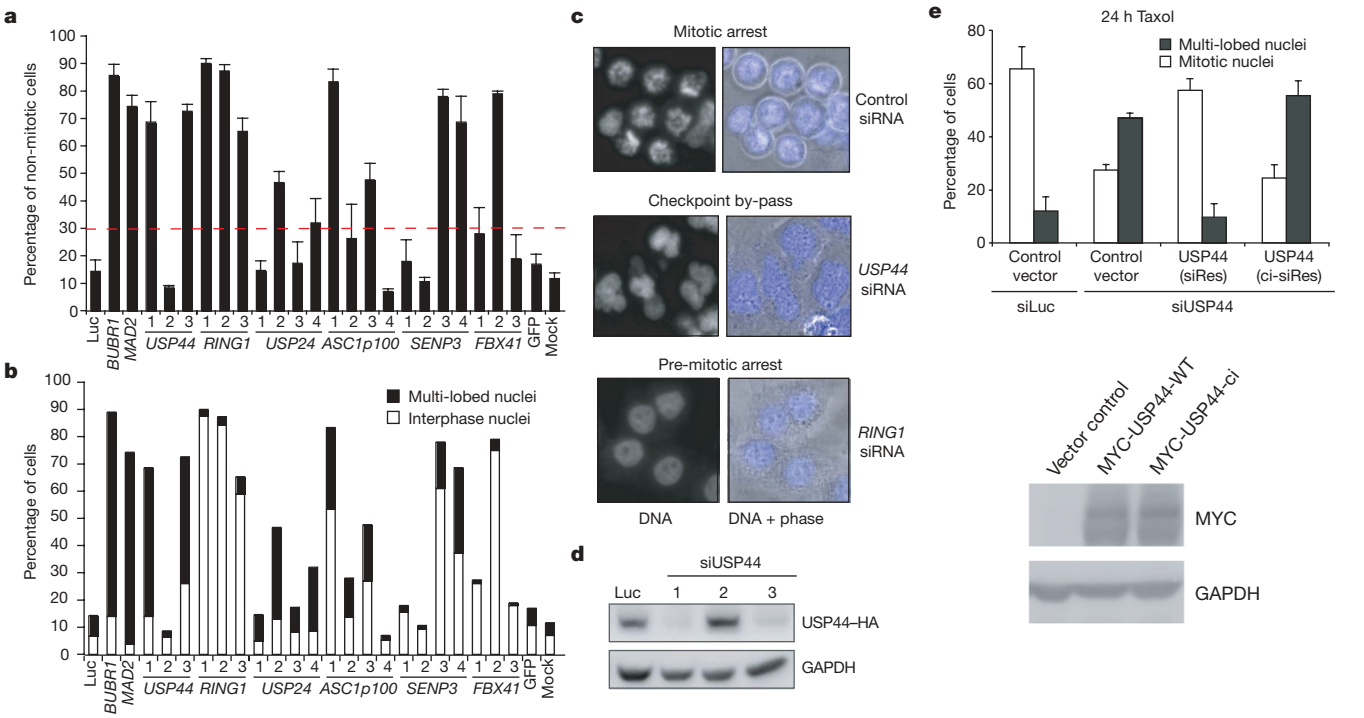

Figure 1 | Validation of candidate genes from Taxol screen. **a**, **b**, HeLa cells were transfected with siRNAs, treated with 100 nM Taxol 48 h after transfection, and fixed for visual inspection 24 h after Taxol addition. The percentage of non-mitotic cells (**a**) and cells with multi-lobed or interphase nuclei (**b**) was quantified. The values represent averages of three independent experiments ($n = 100$, error bars ± 1 s.d.). The horizontal dashed line indicates the applied threshold for Taxol screen (30% non-mitotic cells). **c**, Representative images of HeLa cells transfected with siRNAs targeting luciferase (control), *USP44* (oligo1), or *RING1* (oligo1) that illustrate the phenotypic differences between mitotic arrest, checkpoint by-pass and pre-mitotic arrest. **d**, HeLa cells stably expressing haemagglutinin (HA)-tagged USP44 were transfected with siRNAs, cell extracts collected 48 h after transfection, and probed with the indicated antibodies. **e**, Transfection of siRNA-resistant wild-type Myc-tagged USP44 (USP44(siRes)), but not the catalytically inactive-mutant USP44 (USP44(ci-siRes)), rescues the spindle checkpoint defect of cells treated with *USP44*-targetted siRNA. HeLa cells were transfected with the indicated siRNAs and rescuing plasmids and treated as described for Fig. 1a. Western blot shows similar expression levels of wild-type and mutant Myc–USP44 ($n = 100$; error bars indicate ± 1 s.d.).

©2007 Nature Publishing Group

metaphase plate (fourfold increase), unaligned and lagging chromosomes during anaphase (fivefold and 15-fold increase, respectively), and cytokinesis defects (sevenfold increase) (Fig. 2e, f and Supplementary Fig. 4a). Thus, USP44 has an essential function in an unperturbed cell cycle like other checkpoint proteins[5,6].

When we compared the timing of anaphase onset in cells with reduced USP44, Mad1 or Mad2 function by time-lapse imaging, we found that USP44 depletion markedly accelerated the onset of anaphase, as occurs with reduced levels of Mad2 but not Mad1 (Fig. 2g)[18]. Consistent with accelerated mitotic progression, USP44-depleted cells degraded cyclin B prematurely in prometaphase (Fig. 3a, b), whereas the timing of cyclin A degradation (which is not responsive to checkpoint activation *in vivo*[19,20]) was unaffected (Fig. 3c). These findings, together with the fact that the kinetics of checkpoint by-pass in response to nocodazole treatment were similar in Mad2- and USP44-depleted cells (Supplementary Fig. 4b), indicated that USP44 may control spindle checkpoint function by regulating Mad2.

USP44 regulates Mad2–Cdc20 association

The order of function of spindle checkpoint proteins has been determined by examining their interdependencies of kinetochore recruitment. Currently, all known checkpoint proteins are required for Mad2 localization, placing them upstream of Mad2. By that criterion, USP44 must be downstream of or parallel to Mad2, because Mad2, as well as Bub1, BubR1, Mad1 and Mps1, were all properly localized in USP44-depleted prometaphase cells (Fig. 3d, e and Supplementary Fig. 5).

These results suggest that despite USP44 depletion, cells can detect unattached kinetochores and properly recruit spindle checkpoint proteins. Yet these same cells apparently fail to restrain APC^{Cdc20} activity. APC^{Cdc20} inhibition by the spindle checkpoint is mediated by the direct binding of the stoichiometric inhibitors Mad2 and BubR1 to Cdc20, and their failure to bind APC^{Cdc20} strongly compromises spindle checkpoint function[5–7]. We therefore examined whether USP44-depleted cells are impaired in the formation of these APC-inhibitory complexes. To overcome the problem that USP44-depleted cells do not arrest in response to nocodazole, we used brief proteasome inhibition to arrest synchronized cells in mitosis (for detailed synchronization protocol see Supplementary Fig. 6a). Notably, in the absence of USP44, mitotic APC^{Cdc20} contained significantly reduced levels of co-purifying Mad2 (Fig. 3g and Supplementary Fig. 6b, c). As expected from the reduced Mad2–Cdc20 association, APC^{Cdc20} activity was increased in USP44-depleted cells despite checkpoint activation (Fig. 3f). These findings indicate that cells with reduced levels of USP44 fail to arrest in response to spindle damage because of their inability to maintain Mad2–Cdc20 complexes and consequent failure to restrain APC^{Cdc20} activity. Consistent with this hypothesis, the partial depletion of APC2 (anaphase-promoting complex subunit 2; also called ANAPC2) to levels that did not interfere with mitotic progression of otherwise unperturbed cells (Supplementary Fig. 7d) rescued the checkpoint defect of USP44-depleted cells (Fig. 3h and Supplementary Fig. 7). Together, our findings strongly suggest that USP44 maintains spindle checkpoint arrest by stabilizing the binding of Mad2 to APC^{Cdc20}.

USP44 antagonizes UbcH10-induced APC activation

USP44 might influence APC activity directly or indirectly. If direct, purified USP44 protein should affect APC activity *in vitro*. When

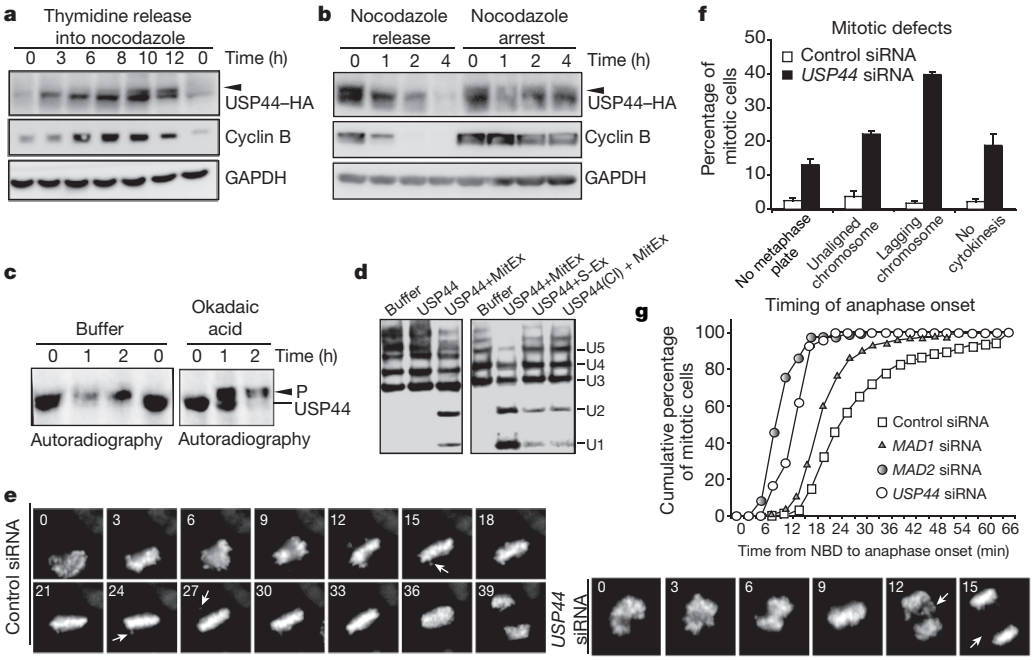

Figure 2 | USP44 activity is cell-cycle regulated and is required for proper spindle checkpoint function and anaphase timing. **a**, HeLa cells stably expressing USP44–HA were released from a double-thymidine block (0 h time point) into medium containing nocodazole. Cell lysates were blotted with the indicated antibodies. The arrowhead marks a slower migrating species of USP44 that is most prevalent in mitotic cells (10 h time point). **b**, HeLa cells stably expressing USP44–HA were synchronized in mitosis (100 ng ml^{-1} nocodazole), 10 mM cycloheximide was added (to prevent *de novo* protein synthesis), and cells were either released from (release) or cultured in the continued presence of nocodazole (arrest). Cell lysates were analysed by western blotting. **c**, Recombinant USP44 is phosphorylated in mitotic extracts. ^{35}S-labelled USP44 was incubated with mitotic extracts and treated either with buffer control or 25 nM okadaic acid (PP2A phosphatase inhibitor). **d**, Recombinant USP44 is activated by incubation with extracts from checkpoint-arrested HeLa cells. Flag-tagged USP44 and USP44(CI) (catalytic inactive, C282A) proteins were purified from insect cells. Where indicated, the bead-bound proteins were incubated for 3 h with mitotic extracts (MitEx) or S-phase extracts (S-Ex). *In vitro* deubiquitination assays using polyubiquitin chains ($Ub_{3–7}$) were performed for 20 min at 37 °C. The migration of monoubiquitin (U1), diubiquitin (U2) and longer ubiquitin chains is indicated. **e–g**, USP44 depletion leads to premature anaphase onset and segregation defects. HeLa cells stably expressing H2B–GFP were transfected with siRNAs and imaged by time-lapse microscopy 48 h after transfection. Times shown are in minutes. Arrows mark uncongressed chromosomes (control siRNA images) and lagging chromosomes (USP44 siRNA images). **f**, Mitotic defects were quantified ($n > 100$, error bars ± 1 s.d.). **g**, The kinetics of anaphase onset was determined by analysing the cumulative percentage of mitotic cells ($n > 100$). NBD, nuclear envelope breakdown.

©2007 Nature Publishing Group

activated USP44 was added to APC^{Cdc20} from checkpoint-arrested cells (CP-APC, which can be activated by the APC-specific E2 UbcH10[21,22]), there was strong inhibition of APC-dependent ubiquitination (Fig. 4a, b and Supplementary Fig. 8a). Notably, USP44 had no effect on ubiquitination reactions catalysed by APC^{Cdh1}, which is not subject to Mad2-mediated spindle checkpoint inhibition (Supplementary Fig. 8b). These findings show that USP44 can directly inhibit APC^{Cdc20} activity.

An accompanying study showed that APC-dependent multi-ubiquitination, but not proteolysis, leads to the disassembly of Mad2–Cdc20 complexes, and identified Cdc20 as a crucial ubiquitination target[16]. Notably, wild-type USP44 but not its catalytically inactive mutant was able to inhibit the UbcH10-driven dissociation of Mad2 from Cdc20 (Fig. 4b, lower panels), which prevented APC^{Cdc20} activation (Fig. 4b, upper panel) and CycB1 degradation (Fig. 4c, d). Moreover, USP44 was very potent at deubiquitinating Cdc20 *in vitro* (Fig. 5a, c, d) and the levels of multi-ubiquitinated Cdc20 increased after USP44 inhibition *in vivo* (Fig. 5e). Consistent with a function for Cdc20 multi-ubiquitination in Mad2–Cdc20 complex disassembly[16], the levels of Mad2 co-purifying with multi-ubiquitinated Cdc20 were substantially reduced in USP44-depleted cells (Fig. 5e). Whilst USP44 was much more efficient at deubiquitinating Cdc20 than cyclin B *in vitro* (Fig. 5a, b), we observed that higher levels of USP44 can promote weak deubiquitination of cyclin B (data not shown). Thus, although pointing towards Cdc20 being the critical target of USP44 that protects cells against premature APC-driven Mad2–Cdc20 complex disassembly, USP44 may additionally antagonize APC function by deubiquitinating other APC substrates.

Given that the APC-driven disassembly of Mad2–Cdc20 complexes requires the function of the E2 enzyme UbcH10 (ref. 16), an implication of our model is that reducing UbcH10 function should suppress the effects of low USP44 activity *in vivo*. In support of this hypothesis, depletion of UbcH10 in cells with reduced USP44 function decreased levels of Cdc20 multi-ubiquitination (Fig. 5e), restored Mad2–Cdc20 association (Fig. 5e), and consequently restored spindle checkpoint arrest (Fig. 5f and Supplementary Fig. 7). In conclusion, our *in vitro* and *in vivo* findings strongly suggest that USP44 directly antagonizes the APC-driven disassembly of Mad2–Cdc20 checkpoint complexes, probably by promoting the deubiquitination of Cdc20. Through the regulation of this ubiquitination–deubiquitination switch, USP44 prevents premature APC activation, which is crucial for proper mitotic timing and spindle checkpoint function.

Discussion

In this study we used a high-throughput shRNA-based forward genetic approach to screen for regulators of the spindle checkpoint and cell-cycle progression in human cells. Our screen identified the first deubiquitinating enzyme (USP44) controlling spindle checkpoint function and revealed a novel mode of APC regulation. USP44 prevents premature APC activation by inhibiting the disassembly of

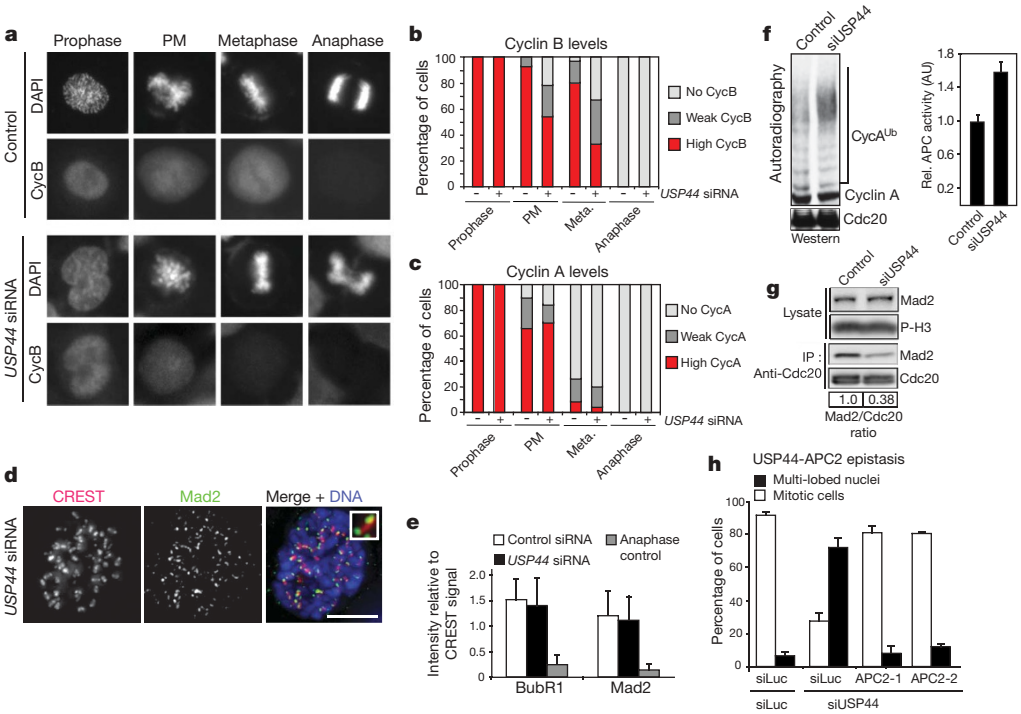

Figure 3 | USP44 regulates APC^{Cdc20} downstream of Mad2 recruitment to kinetochores. **a–c**, USP44-depleted cells prematurely degrade cyclin B but not cyclin A. HeLa cells were treated with siRNAs, synchronized and stained with the indicated antibodies for microscopic analysis. **a**, Representative images of cyclin B staining at different mitotic stages. DAPI, 4,6-diamidino-2-phenylindole; PM, prometaphase. **b**, **c**, Quantification of cyclin A and cyclin B levels ($n > 100$). **d**, USP44 depletion does not impair the localization of Mad2 to unattached kinetochores. Immunofluorescence images of prometaphase cells transfected with siRNAs against *USP44* were probed for Mad2 (green), CREST (red) and stained for DNA (blue). The inset shows the staining of one kinetochore pair at higher magnification. Scale bar, 10 μm. **e**, Quantification of Mad2 and BubR1 levels on prometaphase kinetochores ($n = 150$, error bars ±1 s.d.). **f**, USP44-depleted cells fail to restrain APC^{Cdc20} activation in response to spindle checkpoint activation. HeLa cells were treated with luciferase (control) or *USP44* siRNA, synchronized as described in Supplementary Fig. 6a, and mitotic cells collected by shake-off. Anti-Cdc27 immunoprecipitates (APC^{Cdc20}) were assayed for *in vitro* ubiquitination activity using ^{35}S-labelled cyclin A as a model substrate. The quantification of relative APC activity from three independent experiments is shown on the right (error bars indicate ±1 s.d.). **g**, Mad2–Cdc20 association is reduced after USP44 depletion. Cells were treated as described in **f**. Cdc20 immunoprecipitates and whole-cell lysates were blotted for the indicated proteins. **h**, Partial depletion of APC2 restores spindle checkpoint arrest to USP44-depleted cells. HeLa cells were synchronized and transfected with the indicated siRNAs as described in Supplementary Fig. 7a. Taxol (100 nM) was added after release from the second thymidine block and cells were fixed and stained for DNA (Hoechst) 16 h after release. The percentage of checkpoint-arrested (mitotic cells) and checkpoint-by-passing (multi-lobed nuclei) cells was quantified ($n > 100$, error bars ± s.d.).

©2007 Nature Publishing Group

Mad2–Cdc20 complexes, at least in part by antagonizing APC-dependent multi-ubiquitination of Cdc20 (Supplementary Fig. 9). These findings indicate that spindle checkpoint regulation of the APC is dynamic and based on a fine-tuned balance of counteracting ubiquitination and deubiquitination activities. On the basis of the critical role of USP44 in protecting cells from premature anaphase entry and to establish a common terminology across species, we propose to refer to deubiquitinating enzymes with similar APC antagonizing activities by the general name of 'protectins' (for sequence alignments with potential orthologues in other species, see Supplementary Figs 10 and 11).

In an accompanying study, it was found that the APC itself can drive the disassembly of checkpoint complexes[16]. This feed-forward activation loop provides an elegant mechanism to allow for the rapid activation of APC^{Cdc20} upon cessation of the checkpoint signal. However, it imposes the need for tight regulation before the completion of kinetochore attachment. We propose that protectins such as USP44 provide a critical safeguard mechanism to prevent the inappropriate activation of this feed-forward APC activation loop by antagonizing the multi-ubiquitination of Cdc20 and potentially other components of checkpoint-inhibited APC, thus maintaining the checkpoint-inhibited APC state (Supplementary Fig. 9). Although our data point towards CP-APC and especially Cdc20 as being critical targets of USP44, it is possible that USP44 more broadly antagonizes APC function by de-ubiquitinating other APC substrates such as cyclin B and securin.

An important question is how this ubiquitination–deubiquitination switch is regulated to promote the transition from the checkpoint-inhibited to the active APC state once each chromosome has achieved bipolar attachment. A potential clue comes from our finding that incubation of recombinant USP44 with extracts from checkpoint-arrested but not S-phase-arrested cells strongly increases its activity. How USP44 activity is increased in mitotic extracts is not yet clear. It

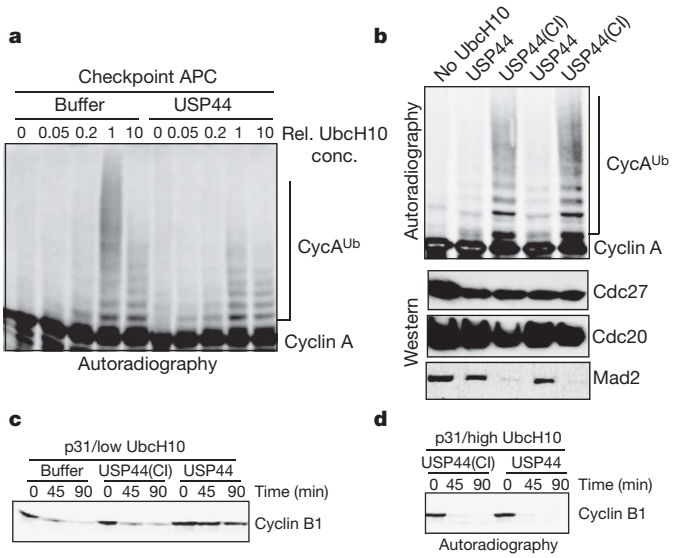

Figure 4 | USP44 inhibits APC^{Cdc20} activation *in vitro*. **a**, USP44 impairs the activation of checkpoint APC by UbcH10 *in vitro*. APC^{Cdc20} was immunopurified from checkpoint-arrested HeLa cells and assayed for *in vitro* ubiquitination activity using ^{35}S-labelled cyclin A as a substrate. UbcH10 and purified USP44 (after activation with mitotic extracts) were added where indicated. **b**, USP44 prevents UbcH10-induced Mad2–Cdc20 dissociation *in vitro*. APC^{Cdc20} was immunopurified from checkpoint-arrested HeLa cells and incubated with UbcH10 and p31 (which triggers Mad2–Cdc20 dissocation[16]) in combination with either wild-type or catalytically inactive USP44 (USP44(CI)). The amount of Mad2 bound to APC^{Cdc20} was determined by western blotting (lower panel), and APC^{Cdc20} activity (top panel) was analysed as described in Fig. 3f. **c**, **d**, USP44 and UbcH10 regulate CP-APC antagonistically *in vitro*. Extracts from checkpoint-arrested HeLa cells were incubated with the indicated proteins and the abundance of ^{35}S-labelled cyclin B was monitored over time by autoradiography. Note that whereas USP44 prevents CP-APC activation (as monitored by cyclin B degradation) induced by low levels of UbcH10 (**c**), fivefold higher levels of UbcH10 can overcome USP44's inhibitory effect (**d**), illustrating their antagonistic relationship.

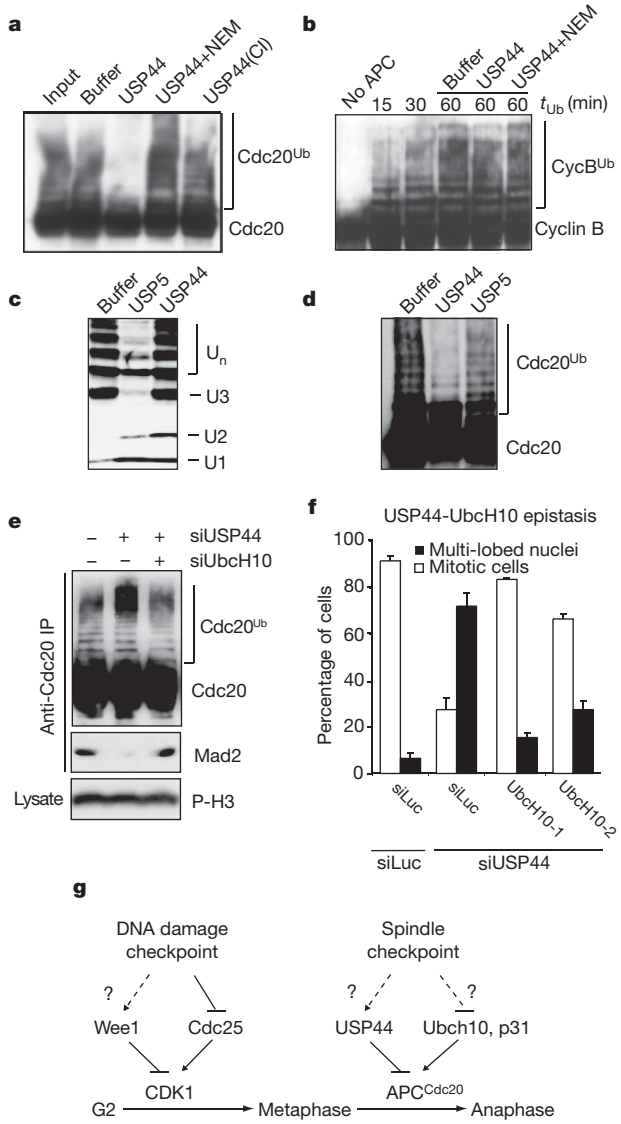

Figure 5 | USP44 deubiquitinates Cdc20 *in vitro* and *in vivo*. **a**, **b**, Ubiquitinated Cdc20 and cyclin B were immunopurified and incubated with USP44 (after activation with mitotic extract), USP44 inactivated by *N*-ethylmaleimide (NEM, a nonspecific deubiquitinating enzyme inhibitor), and USP44 with an active-site mutation (USP44(CI)) for 30 min. The reaction products were analysed by western blotting using anti-Cdc20 (**a**) or anti-cyclin B (**b**) antibodies. **c**, **d**, Comparison of *in vitro* deubiquitination activity of USP44 and USP5. *In vitro* deubiquitination assays using polyubiquitin chains (Ub_{3-7}) and multi-ubiquitinated Cdc20 were performed as described in Fig. 2d and panel **a**. Although USP5 exhibited high activity against free polyubiquitin chains (**c**), it failed to significantly deubiquitinate Cdc20 (**d**) at identical concentrations. **e**, USP44 and UbcH10 regulate Cdc20 multi-ubiquitination and Mad2–Cdc20 association antagonistically *in vivo*. Cells were treated with siRNAs, synchronized as described in Supplementary Fig. 6a, and only mitotic cells collected by shake-off. Cdc20 immunoprecipitates were blotted for the indicated proteins. **f**, Depletion of UbcH10 restores spindle checkpoint arrest to USP44-depleted cells. Cells were synchronized, transfected with siRNAs and treated as described in Supplementary Fig. 7a. The percentage of checkpoint-arrested (mitotic cells) and checkpoint-by-passing (multi-lobed nuclei) cells was quantified ($n > 100$, error bars ± 1 s.d.). **g**, Schematic model that illustrates the analogies between the regulation of entry into mitosis (G2–M transition) and the metaphase–anaphase transition.

©2007 Nature Publishing Group

could require the binding of a coactivator present only in mitotic cells. Alternatively, USP44 might be activated through phosphorylation by mitotic cyclin-dependent kinases or spindle checkpoint kinases. This would be an attractive possibility because it would allow for USP44 activity to be maximal during checkpoint arrest and then be rapidly inactivated once the checkpoint signal has been terminated. The inactivation of USP44, perhaps through dephosphorylation and subsequent degradation, coupled with a simultaneous increase in APC-mediated Cdc20 multi-ubiquitination promoted by UbcH10 and $p31^{comet}$, would trigger feed-forward activation of APC^{Cdc20} and rapid progression into anaphase (Supplementary Fig. 9).

A cell-cycle transition is a unidirectional change of state in which a cell that was performing one set of processes shifts its activity to perform a different set of processes. Inherent properties of these transitions are coordinated antagonistic circuits of positive and negative feedback loops that operate as a switch[23,24]. A well known example of this is the G2 to M transition in which the antagonistic functions of the activating Cdc25 phosphatase and the inhibitory Wee1 kinase regulate Cdk1 (ref. 25). Similarly, exit from mitosis in budding yeast is controlled by the opposing activities of the Cdk1 kinase and Cdc14 phosphatase[26]. No such switch mechanism has been described for the metaphase to anaphase transition, which is controlled by ubiquitination. On the basis of the results of our work and that of ref. 16, we propose that anaphase entry is controlled by a dynamic balance of ubiquitination and deubiquitination, which contributes to the switch-like transition from the checkpoint-inhibited to the active APC state. In this model, p31/UbcH10-stimulated ubiquitination functions analogously to dephosphorylation by Cdc25. Deubiquitination by protectins such as USP44 has a function that is analogous to phosphorylation by Wee1, and APC^{Cdc20} is analogous to Cdk1 (Fig. 5g). These studies illustrate the dynamic interaction between ubiquitination and deubiquitination in controlling key regulatory pathways, and should serve as a basis for future modelling of the metaphase to anaphase transition. We speculate that ubiquitination–deubiquitination switches similar to the one described here might contribute to the generation of bi-stable, switch-like transitions in other biological pathways.

METHODS

See Supplementary Information for full experimental details, including a detailed description of live cell time-lapse imaging and biochemical analyses.

shRNA screen and hit validation. HeLa cells were seeded in 96-well plates (2,000 cells per well) and co-transfected the following day with shRNA-expressing pSM2 plasmids (100–150 ng) and 10 ng dsRed-expressing vector using Exgen 500 (Fermentas). After 48 h, 100 nM Taxol was added and cells fixed with 4% formaldehyde 24 h after Taxol treatment. Cells were scored visually on an inverted microscope (Axiovert 200, Zeiss). The sequences of siRNAs used in this study are listed in Supplementary Table 3.

Cell synchronization. To isolate USP44-depleted mitotic cells, siRNA-transfected cells were synchronized at the G1/S transition by a double thymidine block. To this end, 4 h after siRNA transfection, cells were treated with thymidine (2.5 mM) for 16 h. After releasing cells for 7 h from the first thymidine block, thymidine was re-added for an additional 17 h. Cells were released from the second thymidine block into medium containing 100 ng ml^{-1} nocodazole to trigger spindle checkpoint activation. When cells started to enter mitosis (9 h after release), 10 μM MG132 was added to the medium for the last 2 h before collecting mitotic cells by shake-off (see schematic in Supplementary Fig. 6a).

Received 13 December 2006; accepted 19 February 2007.

1. Lengauer, C., Kinzler, K. W. & Vogelstein, B. Genetic instabilities in human cancers. *Nature* **396**, 643–649 (1998).
2. Draviam, V. M., Xie, S. & Sorger, P. K. Chromosome segregation and genomic stability. *Curr. Opin. Genet. Dev.* **14**, 120–125 (2004).
3. Kops, G. J., Weaver, B. A. & Cleveland, D. W. On the road to cancer: aneuploidy and the mitotic checkpoint. *Nature Rev. Cancer* **5**, 773–785 (2005).
4. Peters, J. M. The anaphase promoting complex/cyclosome: a machine designed to destroy. *Nature Rev. Mol. Cell Biol.* **7**, 644–656 (2006).
5. Musacchio, A. & Hardwick, K. G. The spindle checkpoint: structural insights into dynamic signalling. *Nature Rev. Mol. Cell Biol.* **3**, 731–741 (2002).
6. Bharadwaj, R. & Yu, H. The spindle checkpoint, aneuploidy, and cancer. *Oncogene* **23**, 2016–2027 (2004).
7. Nasmyth, K. How do so few control so many? *Cell* **120**, 739–746 (2005).
8. Hoyt, M. A., Totis, L. & Roberts, B. T. S. *cerevisiae* genes required for cell cycle arrest in response to loss of microtubule function. *Cell* **66**, 507–517 (1991).
9. Li, R. & Murray, A. W. Feedback control of mitosis in budding yeast. *Cell* **66**, 519–531 (1991).
10. Weiss, E. & Winey, M. The *Saccharomyces cerevisiae* spindle pole body duplication gene MPS1 is part of a mitotic checkpoint. *J. Cell Biol.* **132**, 111–123 (1996).
11. Karess, R. Rod-Zw10-Zwilch: a key player in the spindle checkpoint. *Trends Cell Biol.* **15**, 386–392 (2005).
12. Habu, T., Kim, S. H., Weinstein, J. & Matsumoto, T. Identification of a MAD2-binding protein, CMT2, and its role in mitosis. *EMBO J.* **21**, 6419–6428 (2002).
13. Xia, G. *et al.* Conformation-specific binding of p31(comet) antagonizes the function of Mad2 in the spindle checkpoint. *EMBO J.* **23**, 3133–3143 (2004).
14. Mapelli, M. *et al.* Determinants of conformational dimerization of Mad2 and its inhibition by p31comet. *EMBO J.* **25**, 1273–1284 (2006).
15. Kops, G. J. *et al.* ZW10 links mitotic checkpoint signaling to the structural kinetochore. *J. Cell Biol.* **169**, 49–60 (2005).
16. Reddy, S. K., Rape, M., Marganski, W. A. & Kirschner, M. W. Ubiquitination by the anaphase-promoting complex drives spindle checkpoint inactivation. *Nature* advance online publication, doi:10.1038/nature05734 (this issue).
17. Silva, J. M. *et al.* Second-generation shRNA libraries covering the mouse and human genomes. *Nature Genet.* **37**, 1281–1288 (2005).
18. Meraldi, P., Draviam, V. M. & Sorger, P. K. Timing and checkpoints in the regulation of mitotic progression. *Dev. Cell* **7**, 45–60 (2004).
19. Geley, S. *et al.* Anaphase-promoting complex/cyclosome-dependent proteolysis of human cyclin A starts at the beginning of mitosis and is not subject to the spindle assembly checkpoint. *J. Cell Biol.* **153**, 137–148 (2001).
20. den Elzen, N. & Pines, J. Cyclin A is destroyed in prometaphase and can delay chromosome alignment and anaphase. *J. Cell Biol.* **153**, 121–136 (2001).
21. Rape, M. & Kirschner, M. W. Autonomous regulation of the anaphase-promoting complex couples mitosis to S-phase entry. *Nature* **432**, 588–595 (2004).
22. Rape, M., Reddy, S. K. & Kirschner, M. W. The processivity of multiubiquitination by the APC determines the order of substrate degradation. *Cell* **124**, 89–103 (2006).
23. Ferrell, J. E. & Xiong, W. Bistability in cell signaling: How to make continuous processes discontinuous, and reversible processes irreversible. *Chaos* **11**, 227–236 (2001).
24. Markevich, N. I., Hoek, J. B. & Kholodenko, B. N. Signaling switches and bistability arising from multisite phosphorylation in protein kinase cascades. *J. Cell Biol.* **164**, 353–359 (2004).
25. Takizawa, C. G. & Morgan, D. O. Control of mitosis by changes in the subcellular location of cyclin-B1-Cdk1 and Cdc25C. *Curr. Opin. Cell Biol.* **12**, 658–665 (2000).
26. Stegmeier, F. & Amon, A. Closing mitosis: the functions of the Cdc14 phosphatase and its regulation. *Annu. Rev. Genet.* **38**, 203–232 (2004).

Supplementary Information is linked to the online version of the paper at www.nature.com/nature.

Acknowledgements We thank S. Taylor, H. Yu, W. Earnshaw and J. Jin for gifts of reagents; M. Vidal for providing access to their BioRobot platform; S. Lyman and R. King for communicating unpublished results and assistance with the development of the Taxol screening assay; C. Shamu for access to the ICCB-Longwood screening facilities; S. Reddy for helpful comments throughout the course of the work; and T. Westbrook and A. Smogorzewska for their critical reading of the manuscript. F.S. is a fellow of the Helen Hay Whitney Foundation. M.R. is a Human Frontiers Science Program Long-Term Fellow. The siRNA and ICCB-Longwood resources used were funded in part by a NCI grant (T. Mitchison). M.E.S. is an American Cancer Society Postdoctoral Fellow. X.L.A. is an NIH pre-doctoral fellow. M.W.K. thanks the National Institute of General Medical Sciences for its support for the grant Cell Cycle Regulation. This work was supported by grants from NIH and DOD to S.J.E. and by grants from the NIH to J.W.H. S.J.E. is an investigator of the Howard Hughes Medical Institute.

Author Information Reprints and permissions information is available at www.nature.com/reprints. The authors declare no competing financial interests. Correspondence and requests for materials should be addressed to S.J.E (selledge@genetics.med.harvard.edu), J.W.H (wade_harper@hms.harvard.edu), or M.W.K. (marc@hms.harvard.edu).

©2007 Nature Publishing Group